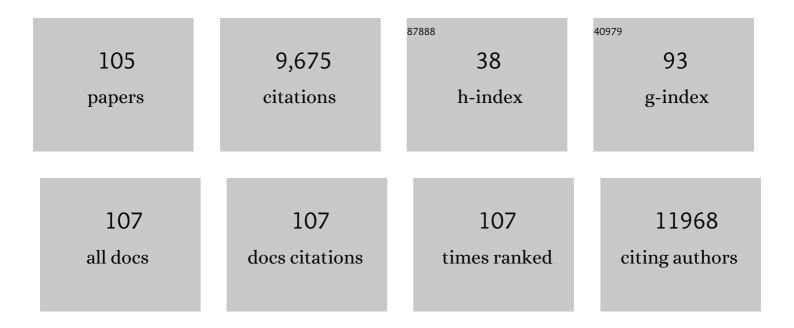
## Bjoern H Menze

List of Publications by Year in descending order

Source: https://exaly.com/author-pdf/9161897/publications.pdf Version: 2024-02-01



#	Article	IF	CITATIONS
1	Face Restoration via Plug-and-Play 3D Facial Priors. IEEE Transactions on Pattern Analysis and Machine Intelligence, 2022, 44, 8910-8926.	13.9	9
2	Modelling glioma progression, mass effect and intracranial pressure in patient anatomy. Journal of the Royal Society Interface, 2022, 19, 20210922.	3.4	5
3	The Medical Segmentation Decathlon. Nature Communications, 2022, 13, .	12.8	252
4	Modeling motor task activation from resting-state fMRI using machine learning in individual subjects. Brain Imaging and Behavior, 2021, 15, 122-132.	2.1	9
5	An automatic multi-tissue human fetal brain segmentation benchmark using the Fetal Tissue Annotation Dataset. Scientific Data, 2021, 8, 167.	5.3	59
6	A computed tomography vertebral segmentation dataset with anatomical variations and multi-vendor scanner data. Scientific Data, 2021, 8, 284.	5.3	22
7	Overdiscrete echoâ€planar spectroscopic imaging with correlated higherâ€order phase correction. Magnetic Resonance in Medicine, 2020, 84, 11-24.	3.0	1
8	Deep neural network for automatic characterization of lesions on 68Ga-PSMA-11 PET/CT. European Journal of Nuclear Medicine and Molecular Imaging, 2020, 47, 603-613.	6.4	66
9	Deep learning-enabled multi-organ segmentation in whole-body mouse scans. Nature Communications, 2020, 11, 5626.	12.8	54
10	Deep-Learning Generated Synthetic Double Inversion Recovery Images Improve Multiple Sclerosis Lesion Detection. Investigative Radiology, 2020, 55, 318-323.	6.2	38
11	Gold Nanoparticle Mediated Multi-Modal CT Imaging of Hsp70 Membrane-Positive Tumors. Cancers, 2020, 12, 1331.	3.7	24
12	Machine learning analysis of whole mouse brain vasculature. Nature Methods, 2020, 17, 442-449.	19.0	203
13	Predicting Clioblastoma Recurrence from Preoperative MR Scans Using Fractional-Anisotropy Maps with Free-Water Suppression. Cancers, 2020, 12, 728.	3.7	23
14	BraTS Toolkit: Translating BraTS Brain Tumor Segmentation Algorithms Into Clinical and Scientific Practice. Frontiers in Neuroscience, 2020, 14, 125.	2.8	50
15	Cellular and Molecular Probing of Intact Human Organs. Cell, 2020, 180, 796-812.e19.	28.9	187
16	Deep complex convolutional network for fast reconstruction of 3D late gadolinium enhancement cardiac MRI. NMR in Biomedicine, 2020, 33, e4312.	2.8	30
17	c-Rel gain in B cells drives germinal center reactions and autoantibody production. Journal of Clinical Investigation, 2020, 130, 3270-3286.	8.2	11
18	A Radiomics Approach to Traumatic Brain Injury Prediction in CT Scans. , 2019, , .		7

2

#	Article	IF	CITATIONS
19	Deep learning derived tumor infiltration maps for personalized target definition in Glioblastoma radiotherapy. Radiotherapy and Oncology, 2019, 138, 166-172.	0.6	28
20	Designing contrasts for rapid, simultaneous parameter quantification and flow visualization with quantitative transient-state imaging. Scientific Reports, 2019, 9, 8468.	3.3	15
21	Cardiovascular Magnetic Resonance-Based Three-Dimensional Structural Modeling and Heterogeneous Tissue Channel Detection in Ventricular Arrhythmia. Scientific Reports, 2019, 9, 9317.	3.3	6
22	Deep Neural Network for Automatic Characterization of Lesions on 68Ga-PSMA PET/CT Images. , 2019, 2019, 951-954.		7
23	Local Conduction Velocity in the Presence of Late Gadolinium Enhancement and Myocardial Wall Thinning. Circulation: Arrhythmia and Electrophysiology, 2019, 12, e007175.	4.8	17
24	Personalized Radiotherapy Design for Glioblastoma: Integrating Mathematical Tumor Models, Multimodal Scans, and Bayesian Inference. IEEE Transactions on Medical Imaging, 2019, 38, 1875-1884.	8.9	96
25	qPSMA: Semiautomatic Software for Whole-Body Tumor Burden Assessment in Prostate Cancer Using <sup>68</sup> Ga-PSMA11 PET/CT. Journal of Nuclear Medicine, 2019, 60, 1277-1283.	5.0	82
26	Differential Diagnosis for Pancreatic Cysts in CT Scans Using Densely-Connected Convolutional Networks. , 2019, 2019, 2095-2098.		19
27	Deep Learning Reveals Cancer Metastasis and Therapeutic Antibody Targeting in the Entire Body. Cell, 2019, 179, 1661-1676.e19.	28.9	142
28	Panoptic imaging of transparent mice reveals whole-body neuronal projections and skull–meninges connections. Nature Neuroscience, 2019, 22, 317-327.	14.8	318
29	Multi-level Activation for Segmentation of Hierarchically-Nested Classes. Lecture Notes in Computer Science, 2019, , 345-353.	1.3	4
30	Multi-scale Convolutional-Stack Aggregation for Robust White Matter Hyperintensities Segmentation. Lecture Notes in Computer Science, 2019, , 199-207.	1.3	1
31	Neural Parameters Estimation for Brain Tumor Growth Modeling. Lecture Notes in Computer Science, 2019, , 787-795.	1.3	11
32	DiamondGAN: Unified Multi-modal Generative Adversarial Networks for MRI Sequences Synthesis. Lecture Notes in Computer Science, 2019, , 795-803.	1.3	36
33	Spatial-Frequency Non-local Convolutional LSTM Network for pRCC Classification. Lecture Notes in Computer Science, 2019, , 22-30.	1.3	0
34	Wall shear stress estimation in the aorta: Impact of wall motion, spatiotemporal resolution, and phase noise. Journal of Magnetic Resonance Imaging, 2018, 48, 718-728.	3.4	23
35	A diffusion modelâ€free framework with echo time dependence for freeâ€water elimination and brain tissue microstructure characterization. Magnetic Resonance in Medicine, 2018, 80, 2155-2172.	3.0	14
36	Why rankings of biomedical image analysis competitions should be interpreted with care. Nature Communications, 2018, 9, 5217.	12.8	198

#	Article	IF	CITATIONS
37	Automatic Multi-Atlas Segmentation for Abdominal Images Using Template Construction and Robust Principal Component Analysis. , 2018, , .		1
38	Direct Estimation of Pharmacokinetic Parameters from DCE-MRI Using Deep CNN with Forward Physical Model Loss. Lecture Notes in Computer Science, 2018, , 39-47.	1.3	16
39	Three-dimensional holographic visualization of high-resolution myocardial scar on HoloLens. PLoS ONE, 2018, 13, e0205188.	2.5	33
40	Impact of Temporal Heterogeneity of Acute Hypoxia on the Radiation Response of Experimental Tumors. Advances in Experimental Medicine and Biology, 2018, 1072, 189-194.	1.6	0
41	How to Exploit Weaknesses in Biomedical Challenge Design and Organization. Lecture Notes in Computer Science, 2018, , 388-395.	1.3	10
42	Automated Whole-Body Bone Lesion Detection for Multiple Myeloma on <sup>68</sup> Ga-Pentixafor PET/CT Imaging Using Deep Learning Methods. Contrast Media and Molecular Imaging, 2018, 2018, 1-11.	0.8	93
43	Brain extraction from normal and pathological images: A joint PCA/Image-Reconstruction approach. NeuroImage, 2018, 176, 431-445.	4.2	20
44	Fully convolutional network ensembles for white matter hyperintensities segmentation in MR images. NeuroImage, 2018, 183, 650-665.	4.2	155
45	Automated Cardiac MR Scar Quantification in Hypertrophic Cardiomyopathy Using Deep Convolutional Neural Networks. JACC: Cardiovascular Imaging, 2018, 11, 1917-1918.	5.3	58
46	Convolutional Neural Networks for Direct Inference of Pharmacokinetic Parameters: Application to Stroke Dynamic Contrast-Enhanced MRI. Frontiers in Neurology, 2018, 9, 1147.	2.4	43
47	DeepASL: Kinetic Model Incorporated Loss for Denoising Arterial Spin Labeled MRI via Deep Residual Learning. Lecture Notes in Computer Science, 2018, , 30-38.	1.3	16
48	Deep Learning with Synthetic Diffusion MRI Data for Free-Water Elimination in Glioblastoma Cases. Lecture Notes in Computer Science, 2018, , 98-106.	1.3	5
49	Btrfly Net: Vertebrae Labelling with Energy-Based Adversarial Learning of Local Spine Prior. Lecture Notes in Computer Science, 2018, , 649-657.	1.3	37
50	Volumetry based biomarker speed of growth: Quantifying the change of total tumor volume in whole-body magnetic resonance imaging over time improves risk stratification of smoldering multiple myeloma patients. Oncotarget, 2018, 9, 25254-25264.	1.8	15
51	An Online Algorithm for Efficient and Temporally Consistent Subspace Clustering. Lecture Notes in Computer Science, 2017, , 353-368.	1.3	0
52	Exploring New Multimodal Quantitative Imaging Indices for the Assessment of Osseous Tumor Burden in Prostate Cancer Using <sup>68</sup> Ga-PSMA PET/CT. Journal of Nuclear Medicine, 2017, 58, 1632-1637.	5.0	33
53	Diffusion tensor image features predict IDH genotype in newly diagnosed WHO grade II/III gliomas. Scientific Reports, 2017, 7, 13396.	3.3	57
54	Quantification of Metabolites in Magnetic Resonance Spectroscopic Imaging Using Machine Learning. Lecture Notes in Computer Science, 2017, , 462-470.	1.3	14

#	Article	IF	CITATIONS
55	SurvivalNet: Predicting patient survival from diffusion weighted magnetic resonance images using cascaded fully convolutional and 3D Convolutional Neural Networks. , 2017, , .		11
56	Segmentation of Skeleton and Organs in Whole-Body CT Images via Iterative Trilateration. IEEE Transactions on Medical Imaging, 2017, 36, 2276-2286.	8.9	12
57	ISLES 2015 - A public evaluation benchmark for ischemic stroke lesion segmentation from multispectral MRI. Medical Image Analysis, 2017, 35, 250-269.	11.6	360
58	Diabetes60 — Inferring Bread Units From Food Images Using Fully Convolutional Neural Networks. , 2017, , .		9
59	Efficient Algorithms for Moral Lineage Tracing. , 2017, , .		6
60	Cell Lineage Tracing in Lens-Free Microscopy Videos. Lecture Notes in Computer Science, 2017, , 3-11.	1.3	8
61	Deep-FExt: Deep Feature Extraction for Vessel Segmentation and Centerline Prediction. Lecture Notes in Computer Science, 2017, , 344-352.	1.3	11
62	Automated processing of webcam images for phenological classification. PLoS ONE, 2017, 12, e0171918.	2.5	7
63	Probabilistic model for 3D interactive segmentation. Computer Vision and Image Understanding, 2016, 151, 47-60.	4.7	Ο
64	A Nonparametric Growth Model for Brain Tumor Segmentation in Longitudinal MR Sequences. Lecture Notes in Computer Science, 2016, , 69-79.	1.3	2
65	Automatic segmentation of abdominal organs and adipose tissue compartments in water-fat MRI: Application to weight-loss in obesity. European Journal of Radiology, 2016, 85, 1613-1621.	2.6	34
66	Human-Drone-Interaction: A Case Study to Investigate the Relation Between Autonomy and User Experience. Lecture Notes in Computer Science, 2016, , 238-253.	1.3	6
67	Cloud-Based Evaluation of Anatomical Structure Segmentation and Landmark Detection Algorithms: VISCERAL Anatomy Benchmarks. IEEE Transactions on Medical Imaging, 2016, 35, 2459-2475.	8.9	127
68	A Generative Probabilistic Model and Discriminative Extensions for Brain Lesion Segmentation— With Application to Tumor and Stroke. IEEE Transactions on Medical Imaging, 2016, 35, 933-946.	8.9	67
69	Stroke Lesion Segmentation Using a Probabilistic Atlas of Cerebral Vascular Territories. Lecture Notes in Computer Science, 2016, , 21-32.	1.3	3
70	Automatic Liver and Lesion Segmentation in CT Using Cascaded Fully Convolutional Neural Networks and 3D Conditional Random Fields. Lecture Notes in Computer Science, 2016, , 415-423.	1.3	332
71	The Minimum Cost Connected Subgraph Problem in Medical Image Analysis. Lecture Notes in Computer Science, 2016, , 397-405.	1.3	3
72	Simultaneous Parameter Mapping, Modality Synthesis, and Anatomical Labeling of the Brain with MR Fingerprinting. Lecture Notes in Computer Science, 2016, , 579-586.	1.3	5

#	Article	IF	CITATIONS
73	Spatially Adaptive Spectral Denoising forÂMRÂSpectroscopic Imaging using Frequency-Phase Non-local Means. Lecture Notes in Computer Science, 2016, , 596-604.	1.3	0
74	The Multimodal Brain Tumor Image Segmentation Benchmark (BRATS). IEEE Transactions on Medical Imaging, 2015, 34, 1993-2024.	8.9	3,589
75	Reconstructing cerebrovascular networks under local physiological constraints by integer programming. Medical Image Analysis, 2015, 25, 86-94.	11.6	19
76	Joint 3-D vessel segmentation and centerline extraction using oblique Hough forests with steerable filters. Medical Image Analysis, 2015, 19, 220-249.	11.6	74
77	Extracting Vascular Networks under Physiological Constraints via Integer Programming. Lecture Notes in Computer Science, 2014, 17, 505-512.	1.3	5
78	Medical Computer Vision: Algorithms for Big Data. Lecture Notes in Computer Science, 2014, , .	1.3	3
79	Multitemporal Fusion for the Detection of Static Spatial Patterns in Multispectral Satellite Images—With Application to Archaeological Survey. IEEE Journal of Selected Topics in Applied Earth Observations and Remote Sensing, 2014, 7, 3513-3524.	4.9	10
80	Radiotherapy planning for glioblastoma based on a tumor growth model: improving target volume delineation. Physics in Medicine and Biology, 2014, 59, 747-770.	3.0	55
81	Radiotherapy planning for glioblastoma based on a tumor growth model: implications for spatial dose redistribution. Physics in Medicine and Biology, 2014, 59, 771-789.	3.0	30
82	Spatio-Temporal Video Segmentation With Shape Growth or Shrinkage Constraint. IEEE Transactions on Image Processing, 2014, 23, 3829-3840.	9.8	64
83	Overview of the 2014 Workshop on Medical Computer Vision—Algorithms for Big Data (MCV 2014). Lecture Notes in Computer Science, 2014, , 3-10.	1.3	0
84	Global localization of 3D anatomical structures by pre-filtered Hough Forests and discrete optimization. Medical Image Analysis, 2013, 17, 1304-1314.	11.6	77
85	Whole-body anatomy localization via classification and regression forests. Medical Image Analysis, 2013, 17, 1282.	11.6	1
86	Sparse Scale-Space Decomposition of Volume Changes in Deformations Fields. Lecture Notes in Computer Science, 2013, 16, 328-335.	1.3	3
87	Enforcing Monotonous Shape Growth or Shrinkage in Video Segmentation. , 2013, , .		4
88	Mapping patterns of long-term settlement in Northern Mesopotamia at a large scale. Proceedings of the United States of America, 2012, 109, E778-87.	7.1	122
89	Automated vs. Manual Pattern Recognition of 3D 1H MRSI Data of Patients with Prostate Cancer. Academic Radiology, 2012, 19, 675-684.	2.5	5
90	Using spatial prior knowledge in the spectral fitting of MRS images. NMR in Biomedicine, 2012, 25, 1-13.	2.8	14

#	Article	IF	CITATIONS
91	A Generative Approach for Image-Based Modeling of Tumor Growth. Lecture Notes in Computer Science, 2011, 22, 735-747.	1.3	45
92	Spatial decision forests for MS lesion segmentation in multi-channel magnetic resonance images. NeuroImage, 2011, 57, 378-390.	4.2	260
93	Detecting stable distributed patterns of brain activation using Gini contrast. NeuroImage, 2011, 56, 497-507.	4.2	61
94	Efficient probabilistic model personalization integrating uncertainty on data and parameters: Application to Eikonal-Diffusion models in cardiac electrophysiology. Progress in Biophysics and Molecular Biology, 2011, 107, 134-146.	2.9	78
95	Multimodal medical image analysis: From visualization to disease modeling. Zeitschrift Fur Medizinische Physik, 2011, 21, 1.	1.5	1
96	Segmentation of image ensembles via latent atlases. Medical Image Analysis, 2010, 14, 654-665.	11.6	64
97	A Generative Model for Brain Tumor Segmentation in Multi-Modal Images. Lecture Notes in Computer Science, 2010, 13, 151-159.	1.3	132
98	A comparison of random forest and its Gini importance with standard chemometric methods for the feature selection and classification of spectral data. BMC Bioinformatics, 2009, 10, 213.	2.6	804
99	Estimating Kinetic Parameter Maps From Dynamic Contrast-Enhanced MRI Using Spatial Prior Knowledge. IEEE Transactions on Medical Imaging, 2009, 28, 1534-1547.	8.9	44
100	Analysing spatio-temporal patterns of the global NO <sub>2</sub> -distribution retrieved from GOME satellite observations using a generalized additive model. Atmospheric Chemistry and Physics, 2009, 9, 6459-6477.	4.9	38
101	Mimicking the human expert: Pattern recognition for an automated assessment of data quality in MR spectroscopic images. Magnetic Resonance in Medicine, 2008, 59, 1457-1466.	3.0	30
102	Robust Prediction of the MASCOT Score for an Improved Quality Assessment in Mass Spectrometric Proteomics. Journal of Proteome Research, 2008, 7, 3708-3717.	3.7	182
103	Automated estimation of tumor probability in prostate magnetic resonance spectroscopic imaging: Pattern recognition vs quantification. Magnetic Resonance in Medicine, 2007, 57, 150-159.	3.0	43
104	Multivariate feature selection and hierarchical classification for infrared spectroscopy: serum-based detection of bovine spongiform encephalopathy. Analytical and Bioanalytical Chemistry, 2007, 387, 1801-1807.	3.7	55
105	Detection of Ancient Settlement Mounds. Photogrammetric Engineering and Remote Sensing, 2006, 72, 321-327.	0.6	75